JOURNAL OF AIRCRAFT
Vol. 41, No. 1, January–February 2004

Swept-Wing Outboard-Horizontal-Stabilizer Aircraft Configuration

J. A. C. Kentfield* and Adam Spragins†
University of Calgary, Calgary, Alberta T2N 1N4, Canada

The concept of a high-subsonic Mach-number, swept-wing, aircraft configuration with outboard horizontal stabilizers (OHS) was investigated experimentally by means of wind-tunnel tests. Because the wind-tunnel model employed airfoil surfaces with symmetric sections, additional theoretical work was carried out to investigate the influence on OHS flight performance of substituting wings of asymmetric section as often used for so-called supercritical airfoils designed for high-subsonic Mach-number flight. Such airfoils generate significant negative pitching-moment coefficients. The wind-tunnel tests showed that the OHS concept works very well with substantial drag-reduction benefits, relative to conventional configurations, essentially equal to those previously demonstrated for nonswept wing OHS vehicles. It was found, from the theoretical treatment, that the introduction of a negative pitching moment degraded the performance, in terms of lift/drag ratio, of both OHS and corresponding conventional aircraft but the OHS arrangement retained a substantial overall superiority.

Nomenclature

a	=	downwind displacement of c.g. from (mean aerodynamic chord)/4
c	=	chord dimension (measured at mean-aerodynamic-chord location)
C_L	=	lift coefficient (three-dimensional case)
C_l	=	two-dimensional wing lift coefficient
C_M	=	pitching-moment coefficient (nose-up positive)
D	=	drag of aerodynamic surfaces
L	=	lift of all aerodynamic surfaces
L'	=	distance from $c_w/4$ to $c_{\mathrm{TH}}/4$
X	=	distance from leading edge of aerodynamic surface
α	=	angle of incidence of an airfoil
$\bar{\alpha}$	=	average angle of incidence with wing washout (or twist)
χ	=	distance, as a fraction of c_w, from leading edge

Subscripts

ac	=	aerodynamic center (at mean-aerodynamic-chord station)
$c/4$	=	quarter-chord (at mean-aerodynamic-chord station)
TH	=	horizontal stabilizer
W	=	wing

Introduction

AN OUTBOARD-HORIZONTAL-STABILIZER (OHS) aircraft configuration is one in which a pair of horizontal-stabilizer aerodynamic surfaces are carried outboard, and downwind, of the wing tips. This places them in the upwash flows generated by the wing, which offers the potential for them to serve as efficient lifting surfaces. For it to be feasible for the horizontal tail surfaces to generate lift, as distinct from zero lift or a small negative lift, the c.g. of an OHS aircraft will be significantly further aft than the 25 to 30% of the wing mean aerodynamic chord (MAC) of typical conventional aircraft. For an OHS configuration the c.g. will likely be in the region of the 65% wing MAC station or even further aft. The tail surfaces on an OHS aircraft can, therefore, be supported on booms projecting downwind from each wing tip of a monoplane, or wing tips if a biplane OHS configuration is contemplated. Each boom will, conveniently, also support a vertical stabilizing surface.

For the horizontal tail surfaces to retain their conventional role in pitch control, it is essential that the maximum tail lift coefficient C_{LTH} be substantially less, under all flight conditions, than that which would cause the tail surfaces to stall. Hence, if the wing stalls the horizontal tail surfaces will not stall nor will they stall under any other flight condition. Because the lift generated by the horizontal stabilizers of an OHS configuration is additional to that of the main wing, the wing area of an OHS configuration will be less than that of a conventional aircraft of equal gross lift. The tail of a conventional aircraft generates, typically, no lift or a negative lift.

The expectation of the efficient generation of lift from the horizontal tail surfaces is based upon the nature of the flow, downwind of the wing tips, approaching these surfaces. This flow has an upwash component, which results in the tail-lift vectors being tilted forward and thereby serving to help cancel the drag of the horizontal stabilizers. This feature has been demonstrated both experimentally and analytically.[1,2] Furthermore, the wing-tip-generated flow is also inclined inwards towards the tail vertical surfaces, thereby generating, in a horizontal plane, an aerodynamic lift force that also helps to cancel the aerodynamic drag of these surfaces.[1,2] In fact, it can be shown that for most flight conditions the flow inclinations to the tail surfaces result in a complete cancellation of tail drag and the generation of a net thrust from the tail surfaces.

For flight at high-subsonic Mach numbers, the wings and lifting tail surfaces of an OHS aircraft should be swept to suppress the development of significant regions of supersonic flow. For the case of the wings of an OHS configuration, the wings should be swept forward, relative to the fuselage, to preserve structural stability. This situation is opposite to that prevailing for conventional high-subsonic Mach-number aircraft. Figure 1 illustrates, diagrammatically, an OHS configuration with a modest forward-sweep angle of 15 deg, applied to a uniform chord wing, suitable for a fairly high subsonic flight Mach number.

A prime purpose of the work reported here was to obtain subsonic, low-speed, wind-tunnel test results for a swept-wing OHS configuration and an otherwise comparable vehicle with a conventional central tail. These results were to be compared with available data from earlier, corresponding model tests with a nonswept wing.[1] Because the earlier tests were conducted using a symmetrical-section wing, the tests reported here were also conducted using a wing of symmetrical section. An additional major objective was to carry out a similar analysis to that done experimentally, by theoretical means for a much higher wing-chord-based Reynolds number. This work, which was independent of the wind-tunnel tests, was also for wings

Received 22 January 2003; revision received 23 May 2003; accepted for publication 24 May 2003. Copyright © 2003 by the American Institute of Aeronautics and Astronautics, Inc. All rights reserved. Copies of this paper may be made for personal or internal use, on condition that the copier pay the $10.00 per-copy fee to the Copyright Clearance Center, Inc., 222 Rosewood Drive, Danvers, MA 01923; include the code 0021-8669/04 $10.00 in correspondence with the CCC.

*Professor, Member AIAA.
†Summer Student, Department of Mechanical and Manufacturing Engineering, 2500 University Drive N.W.

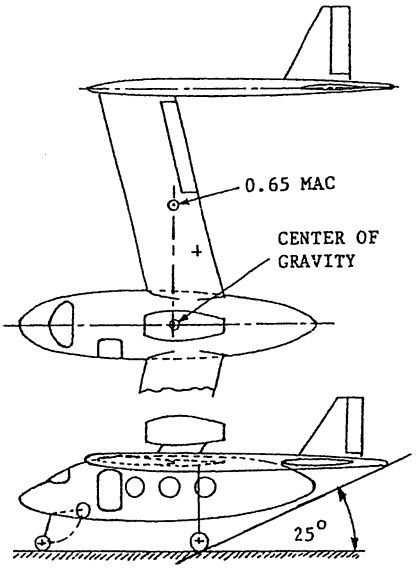

Fig. 1 OHS light, single jet, transport aircraft for a high-subsonic cruise Mach-number (diagrammatic).

of symmetric section. The final requirement was to adapt the analytical treatment to represent wings of asymmetric section having large wing-pitching-moment coefficients representative of the pitching-moment coefficients of generic supercritical wings likely to be used for high subsonic Mach-number aircraft employing wing sweep. In terms of the results reported here, the major difference between a conventional symmetric wing and a supercritical wing was expected to be the negative pitching moment of the latter. Details of the lift and drag vs incidence angle relationships of supercritical wings were not a prime interest of the study.

The type of OHS aircraft described here was not the first form of air vehicle with the horizontal, or essentially horizontal, tail surfaces outboard of the wing tips. Descriptions of some of the earlier work can be found elsewhere.[2,3]

Theoretical Considerations

The main reason for the use of forward-swept wings in OHS aircraft is to achieve structural stability. This is essentially the same as the reason for employing aft-swept wings in conventional, high subsonic Mach-number aircraft. In both cases the wings are swept rearwards relative to the pitch-stabilizing surfaces provided. For the OHS case these are attached to the downwind ends of the booms, which are, themselves, secured to the wing tips. For conventional configurations the pitch-stabilizing horizontal tail is mounted at the downwind end of the fuselage. In this case a transient upload on the wing tends to produce, because of a classical bending and torsion action, a torque that decreases the wing-tip angle of attack. With an OHS configuration a transient wing upload produces a torque tending to reduce the wing angle of attack near the central fuselage, which tends, as a result, to tilt the fuselage slightly nose down. In both cases the opposite effects are noted with transient downloads or load reductions.

A convenient feature of forward sweep in conjunction with a relatively far aft c.g. location is, as can be seen from Fig. 1, that it is possible to provide fuel tankage effectively centered on the aircraft c.g. in the inboard portions of the wing. Another possible location for fuel tankage is in the booms supporting the tail surfaces. Generally, the feasibility of wing fuel tankage located symmetrically fore and aft of the aircraft c.g. depends upon the aircraft aspect ratio, wing sweep angle, and the extent of the aft-setting of the c.g. on the wing MAC line. Forward wing sweep also has the effect, in some cases, of making it possible to attach the main undercarriage to the wing.

The tail surfaces, which for OHS configurations are aerodynamic lifting surfaces, are provided with conventional rearward-swept leading edges. The rearward sweep should also help minimize the need for twisted tail surfaces. The rearward sweep will contribute to increasing the effective angle of incidence towards the outboard tips of these surfaces while permitting a reduction of incidence closer to the boom attachment locations, thereby reducing the likelyhood of stall close to the booms.

Although the wind-tunnel tests were conducted using a symmetrical cross section wing of NACA-0018 cross-section normal to the leading and trailing edges of the wing (NACA-00163 parallel to the freestream direction), a high subsonic Mach-number vehicle will very likely employ a supercritical or near supercritical, airfoil section. This is likely to have a relatively large (negative) pitching moment $C_{M/(\mathrm{ac})}$ about the aerodynamic center. This will, therefore, result in the airfoil center of pressure moving progressively rearwards with reduction of the airfoil lift coefficient C_l as per the well-known relationship

$$\chi_{\mathrm{cp}} = \chi_{\mathrm{ac}} - C_{M/(\mathrm{ac})} \big/ C_l \tag{1}$$

where χ_{cp} and χ_{ac} are expressed as fractions of the wing chord c_w, thus making the following approximations for the constant chord wing: $C_l \cong C_L$, that is, wing loading approximates an elliptic condition where $C_l = C_L$ and $C_{M(\mathrm{ac})} \cong C_{M(c/4)}$ also

$$\chi_{\mathrm{ac}} \cong X_{c/4}/c_w, \qquad \chi_{\mathrm{cp}} = X_{\mathrm{cp}}/c_w$$

Equation (1) becomes

$$X_{\mathrm{cp}}/c_w \cong X_{c/4}/c_w - C_{M(c/4)} \big/ C_L \tag{2}$$

The rearward movement of the wing center of pressure as C_L is reduced identifies the main difference in terms of the work reported here between the conditions applicable to the wind-tunnel tests and those expected to be applicable to an actual high-subsonic Mach-number aircraft. A rearward movement of the wing center of pressure is also to be expected when an otherwise symmetric airfoil is equipped with a flap. Here, however, operation with the flaps deployed at a low value of C_L is not a realistic operating condition. It is because of this rearward movement of the center of pressure that has been found, from earlier work with nonswept wings, to render the use of a flap on the lifting horizontal tails of OHS aircraft unnecessary.[4]

Wind-Tunnel Apparatus

The wind-tunnel tests reported here were carried out in the open-jet facility that was used for earlier tests with nonswept wings. Accordingly, the same NACA-0018 wing, as used for the earlier work, was modified by cutting the original solid-wood wing to provide, after reassembly, a nontapered wing with 25-deg forward sweep as illustrated in Fig. 2. The aspect ratio of the modified wing was 4.98 or, with the inclusion of the wing extensions because of the tail support booms, 5.18. The width of the modified NACA-0018 section measured in the freestream direction was 16.3%. The planform areas of the original nontapered, nonswept, and the modified swept wing were equal. The selection of a 25-deg sweep angle was typical of the $\frac{1}{4}$-chord aft-swept angles of several high-subsonic Mach-number aircraft, for example, the Boeing 737, McDonnell Douglas DC-8 and DC-9, and several Dassault executive jets. The wind-tunnel blockage caused by the model was, for the most extreme operating condition, less than 3.5% of the tunnel flow cross-sectional area.

The wind-tunnel tests of the forward-swept wing with the conventional, centrally located, aft-tail assembly were undertaken merely for the purpose of comparison with the corresponding results for the forward-swept-wing OHS configuration. A heavily forward-swept wing used in conjunction with a conventional aft tail would normally be expected to be structurally unstable because of a coupled bending and torsional affect in a full-scale unit with an elastic wing structure. However no such structural instability was noted with the relatively rigid solid-wood wing of the wind-tunnel model.

A typical wing-chord-based Reynolds number of approximately 6.5×10^4 was representative of the wind-tunnel tests. The planform area of the horizontal stabilizers of the wind-tunnel model was a total of approximately 40% of the wing planform area. The two vertical surfaces totalled a projected area equal to approximately 30%

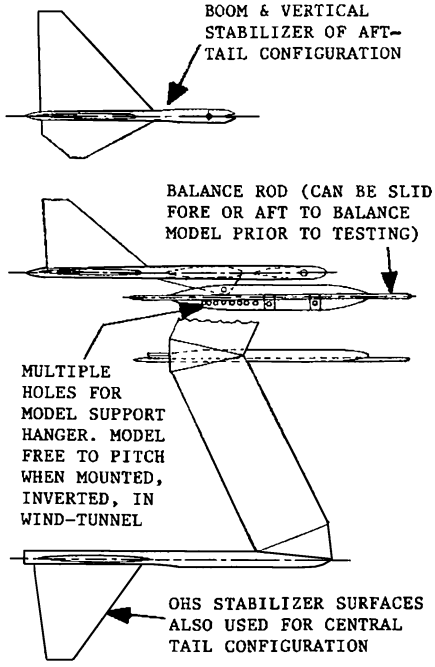

Fig. 2 Wind-tunnel model for low-speed tests of an OHS configuration with 25 deg of forward wing sweep and also for testing a swept-forward configuration with a central tail.

of the wing planform area. The single, central, vertical stabilizer of the conventional aft-tail version of the wind-tunnel model also had a planform area equal to approximately 30% of the main-plane planform area. The thickness of the tail surfaces were typically about 12% of their MAC.

Relative to the earlier tests with a nonswept wing,[1] the length of the OHS booms were increased, and that of the central boom decreased, to maintain for the forward-swept wing tests the same tail moment-arm lengths that prevailed for the earlier tests.[1] The span of the model over the tips of the horizontal stabilizers was 0.75 m (29.5 in.), and the cross section of the open-jet wind-tunnel flow stream was 1.372 m (54 in.) width by 0.762 m (30 in.) height. The model was tested, for convenience, inverted in the tunnel. The model was supported on a pivotted mount on the lift balance such that it was free to rotate in pitch. The model was balanced about the selected pivot location on the model by means of adjustment, fore or aft, of the balance rod shown in Fig. 2 to set the fuselage of the model horizontal. The horizontal setting of the fuselage of the model was maintained, during each test, by adjustment of the incidence angle of the all-flying horizontal stabilizers. Prior to each test, the wing incidence angle, relative to the fuselage, was set to the desired wing incidence angle for that particular test.

Wind-Tunnel Test Results

Results for the forward-swept OHS configuration are shown in Fig. 3 in terms of configuration lift/drag (L/D) vs incidence angle α. Corresponding data for a centrally located tail forward-swept-configuration are shown in Fig. 4. The pivot location at which the model was supported was, for Fig. 3, 0.65 of the wing MAC aft of the wing leading edge, and for Fig. 4 the support location was 0.28 of MAC aft of the wing leading edge. Figure 5 presents a comparative plot of the results obtained. It can be seen that the OHS configuration produces results typically about 17 to 20% better, in terms of L/D, than those obtained with the central, conventional, tail.

Unfortunately there is substantial data scatter apparent in Figs. 3 and 4. This was caused, primarily, by a lack of experience on the part of the data collector. However, to some extent the consequences were mitigated by virtue of the large number of data points gathered. In any case the results presented in Figs. 3 and 4, and also Fig. 5, were later superceded by those of Figs. 11–13. The results presented in the latter diagrams were obtained by a more experienced worker

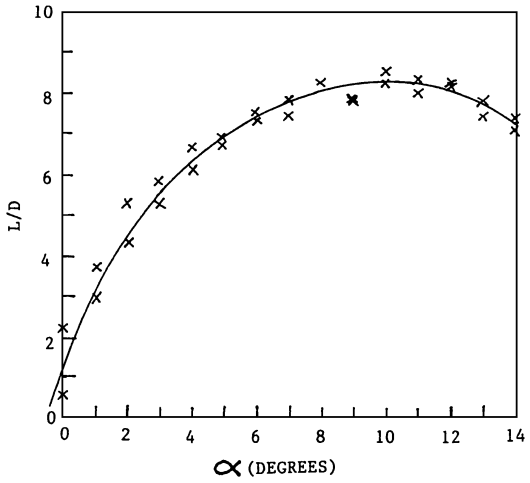

Fig. 3 Lift/drag versus incidence angle α for forward-swept OHS configuration.

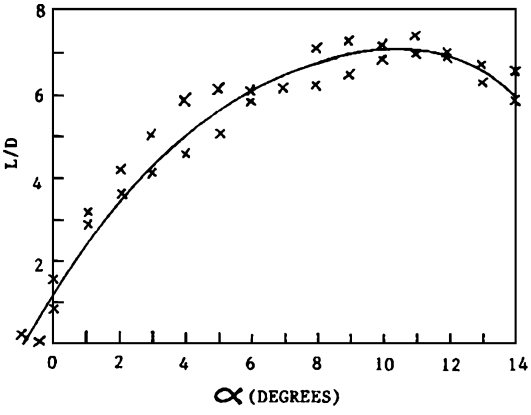

Fig. 4 Lift/drag vs incidence angle α for forward-swept configuration with traditional central tail assembly.

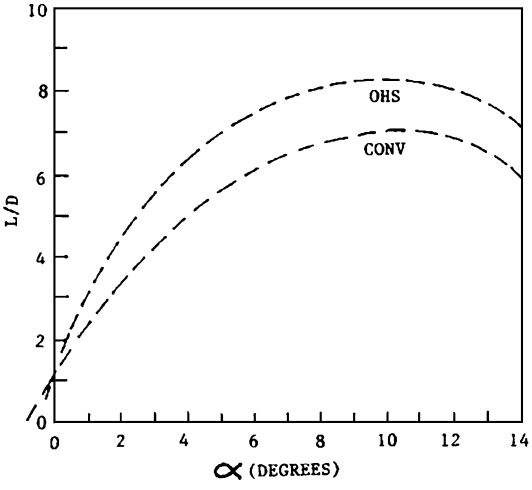

Fig. 5 Comparison of data from Figs. 3 and 4 showing the superior L/D values of the OHS configuration.

revealing an accuracy in the individual measurement of L/D values of approximately ± 0.2 of an L/D unit regardless of the absolute L/D value. Considering the overall complexity of the combined series of interactive measurements, namely, three angular measurements plus separate lift-and-drag measurements, the apparent overall accuracy of Figs. 11 and 12, and hence Fig. 13, appears to be reasonably acceptable.

A test was also conducted on the OHS configuration with the addition of a simple, full-span, flat, "zap-like" flap added to the wing

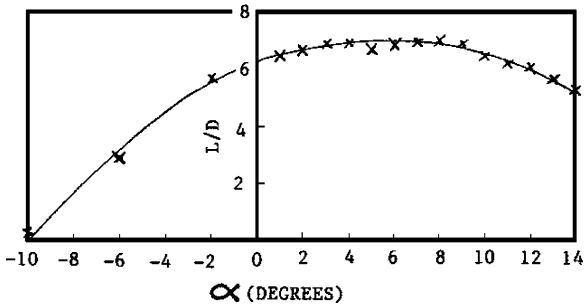

Fig. 6 Lift/drag vs incidence angle α for wind-tunnel model with $0.18c_w$ full-span flaps set at 25 deg to leading and trailing edges of wing of OHS configuration.

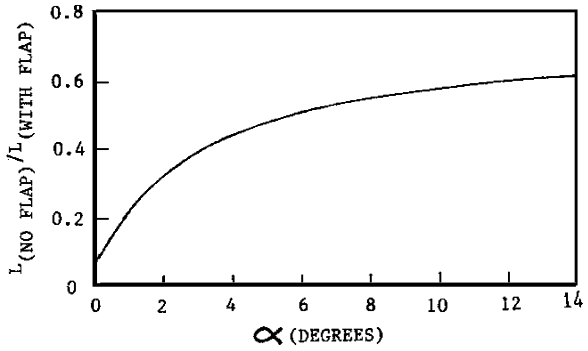

Fig. 7 Ratio of net lifts of wind-tunnel model with and without the full-span flap of Fig. 9.

trailing edge. A zap flap is similar to a split flap with the exception that the hinge location tracks rearwards to the wing trailing-edge station when deployed. This flap had a chord of 18% of that of the swept wing (or 20% of the width from the leading to the trailing edge of the wing measured normal to the wing leading edge). The flap was deflected 25 deg normal to the wing leading and trailing edges (i.e., at 25 deg to the chord line of the nonswept wing). The results obtained with the flap deployed are presented in terms of L/D vs incidence angle in Fig. 6 and in terms of lift increment in Fig. 7. It is clear from Fig. 7, that the flap increased the lift of the model by a minimum of 40% at high angles of incidence with, of course, equal dynamic pressures.

A special hanger, free to swivel in the yaw direction, was employed to support the model to investigate yaw stability with the flap deployed. It was suspected that the use of a flap in conjunction with a forward-swept wing trailing edge could result in a yaw instability. It was found that this expectation was, at least for the configuration tested, unfounded. Not only did the model remain aligned with the oncoming flow, but when the model was perturbated in a yaw direction it promptly realigned with the flow.

Wing Flow-Separation

The comparatively small benefit accruing from the OHS configuration relative to the performance of the swept wing with the centrally located tail compared with the relative benefit of the OHS configuration with nonswept wings noted in earlier work[1] suggested the possibility that flow could, perhaps, be separating from the inner portion of the wing suction surface. Such flow separation would be likely to hurt the performance of the OHS configuration, but for the configuration with the centrally located tail assembly the horizontal stabilizers might well help to generate lift in a compensatory manner. Accordingly a simple flow-visualization test served to confirm a significant area of flow separation at an incidence angle of 10 deg as represented in Fig. 8. It was felt that this problem was caused, primarily, by the swept nature of the wing and was exacerbated by the low Reynolds number of the wind-tunnel tests.

Accordingly, in order to introduce a measure of washout towards the center of the solid-wood wing the wing was cut, as shown in Fig. 9, to introduce a discontinuous washout step by means of which

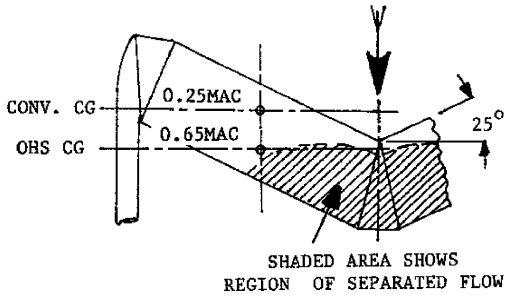

Fig. 8 Region of flow separation of model forward-swept wind-tunnel wing at 10-deg angle of incidence.

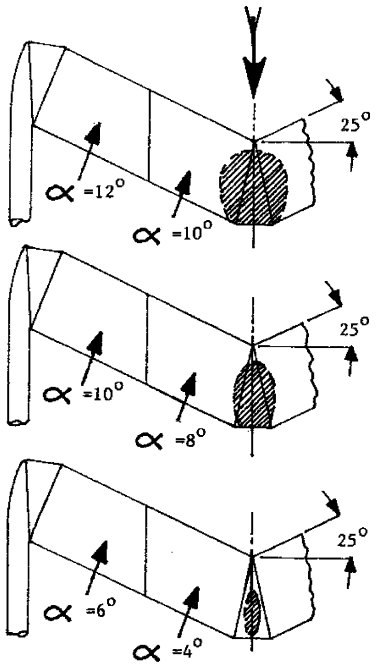

Fig. 9 Reduced regions of flow separation with simulated 2-deg washout from wing-tip towards aircraft centerline.

the wing was effectively twisted by 2 deg at the location shown. The results of this modification are presented in Fig. 9 showing that the area of separated flow was reduced significantly compared with results shown in Fig. 8. A further cut, or slice, at the inboard location depicted in Fig. 10, was provided with an additional 1 deg of washout for the wing center section. This cured, effectively, the wing flow separation problem, and the modified wing configuration shown in Fig. 10 was employed for the remainder of the tests with the forward-swept wing.

Test with Wing Washout

The results of tests with 3 deg of wing washout from the boom toward the central fuselage are presented in Figs. 11–13. The new results for the OHS configuration are presented in Fig. 11. The effective angle of incidence, $\bar{\alpha}$ deg at 0 deg, corresponds to a positive angle of incidence of 1 deg for the outer wing panels with a negative angle of incidence of 1 deg for the adjacent, inner panels and a negative incidence angle of 2 deg for the small, innermost, central portion of the wing. It is probably this situation that leads to an L/D ratio of 2 at a zero value of $\bar{\alpha}$. The peak L/D value was found to be approximately 9.2 at a value of $\bar{\alpha} = 10.5$ deg. This value is slightly less than the peak value of 9.5 realized from earlier tests with a nonswept wing[1] but is significantly greater than the value of 8.2 at $\alpha = 10$ deg obtained with the nontwisted forward-swept wing.

The performance obtained with the swept-forward wing with washout from the boom station to the central fuselage is shown, with the centrally located tail, in Fig. 12. The averaged angle of

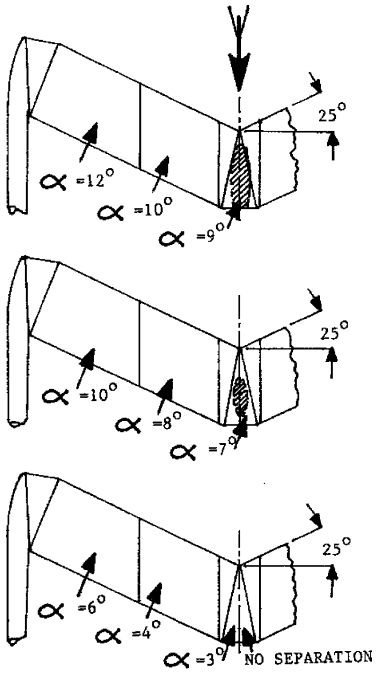

Fig. 10 Reduced regions of flow separation with simulated 3-deg washout from wing tip towards aircraft centerline.

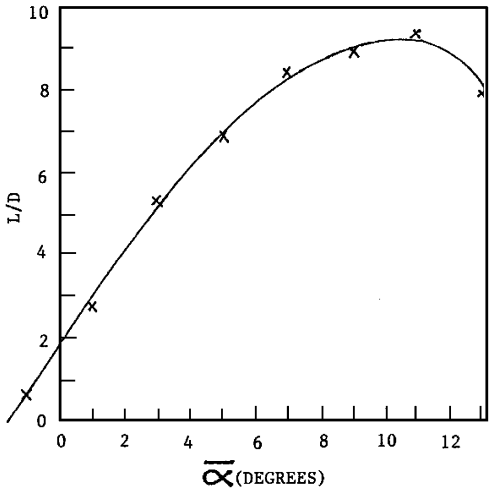

Fig. 11 Lift/drag vs effective average incidence angle $\bar{\alpha}$ for OHS configuration with 3-deg of wing washout.

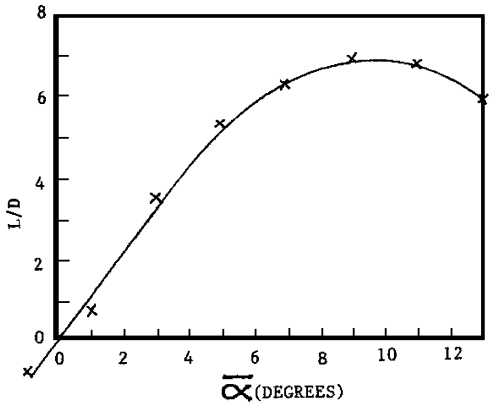

Fig. 12 Lift/rag vs effective average incidence angle $\bar{\alpha}$ with 3 deg of wing washout and traditional central tail assembly.

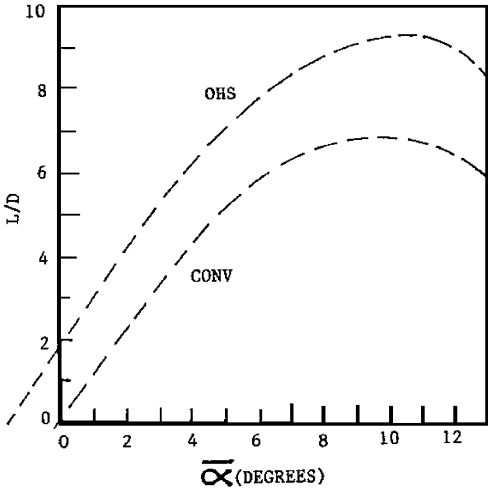

Fig. 13 Comparison of data from Figs. 6 and 7 showing the significantly superior L/D values of the OHS configuration.

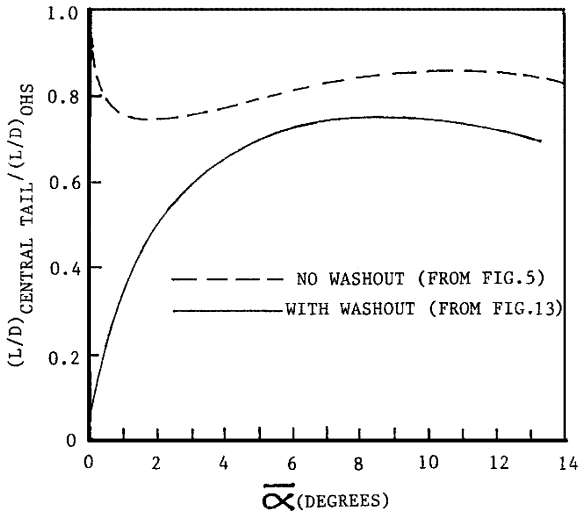

Fig. 14 Comparison of lift/drag ratios for twisted and nontwisted, swept-forward wings (data from wind-tunnel tests).

incidence $\bar{\alpha}$ was defined in the same way as for Fig. 11. The wing performance is slightly poorer than that shown in Fig. 4 for the nontwisted swept-forward wing. The maximum value of L/D for the twisted wing is approximately 6.8 at the effective spanwise averaged angle of incidence $\bar{\alpha}$ of 9.5 deg. This value is slightly less than the corresponding maximum L/D value of 7.0 at an incidence angle of about 9 deg that was achieved before with the nonswept wing.[1]

A comparison of the results achieved with the twisted, forward-swept wing is shown in Fig. 13. The ratio of the peak values of L/D obtained with the twisted, swept-forward wing was approximately 0.74, the same as the value found earlier[1] with the nonswept, nontwisted wing, showing that the peak L/D values with a central tail configuration were only about $\frac{3}{4}$ of the corresponding values obtainable with an OHS configuration for both nonswept and swept-forward wings when the latter are provided with suitable washout. Figure 14 presents a comparison of the performances with twisted and nontwisted swept-forward wings. The dashed curve of Fig. 14 was derived from Fig. 5 and the solid curve from Fig. 13.

Use of a Supercritical Wing

The wind-tunnel tests described here were based on a symmetrical wing section. This was an essential feature in order to compare, in an equitable manner, the influence of wing sweep on the behavior of OHS configurations with available data, obtained earlier,[1] for nonswept-wing OHS configurations. However any high-subsonic

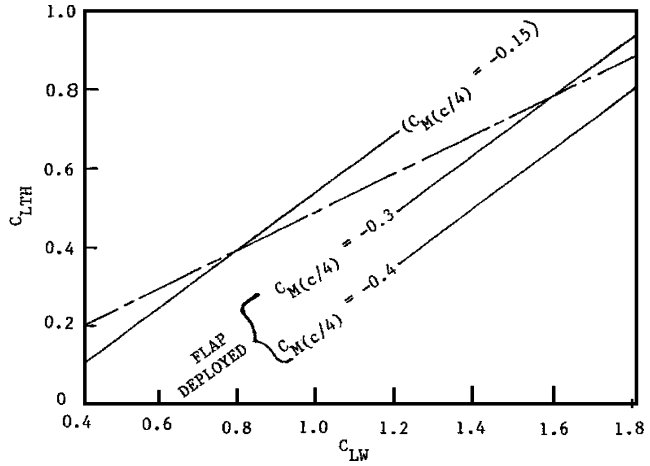

Fig. 15 Horizontal stabilizer, lift coefficient C_{LTH} vs wing lift coefficient C_{LW} for symmetric wing sections and corresponding data for asymmetric wings (from theoretical analysis).

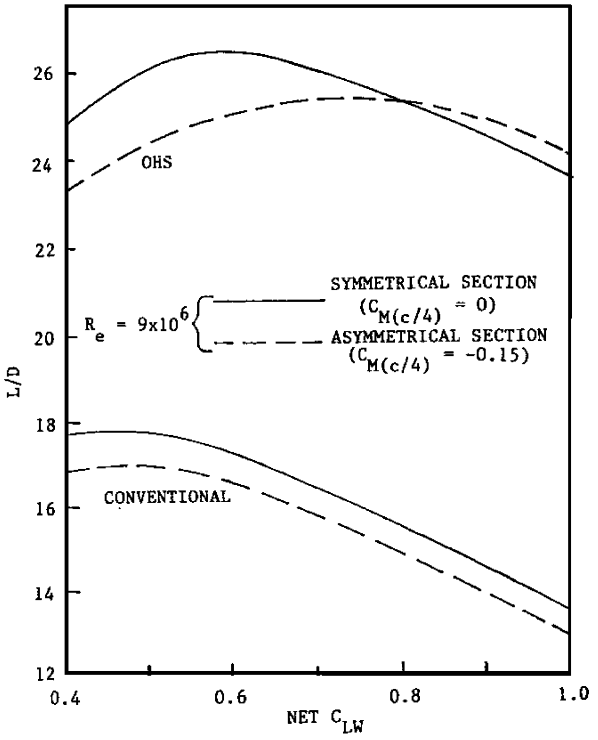

Fig. 16 Theoretically derived lift/drag ratios for OHS and conventional configurations with symmetric and asymmetric airfoil sections: wing aspect ratio = 6, effective horizontal stabilizer aspect ratio = 8, wing-chord-based Reynolds number $\cong 9 \times 10^6$.

Mach-number aircraft will probably employ a so-called supercritical wing section that will almost certainly have a large negative-moment coefficient as distinct from the zero-moment coefficient of a classical symmetric section. The use of flaps will render a symmetrical airfoil section temporarily asymmetric during flap deployment with a consequence that the center of pressure moves rearwards as a result of the generation of a negative pitching-moment coefficient as described in Eq. (2). However flap deployment occurs, normally, only at high lift coefficients, and this effect can usually be accommodated quite easily by OHS configurations. A longer duration, and potentially more troublesome, situation occurs towards the end of a period of cruise flight when the wing lift coefficient is relatively low ($C_{\mathrm{LW}} \cong 0.4$) and a wing of asymmetric section is employed, such as a so-called supercritical wing. A comparison was, therefore, made between the performances of the aerodynamic surfaces of OHS vehicles employing symmetric wing and tail sections with an alternative design in which the wing was assumed to have a negative moment representative of a generic supercritical wing. On the basis of the coordinates of Fig. 15, the prime difference in performance characteristics between a symmetric wing section and an asymmetric section of equal aspect ratio is the large negative pitching moment of the latter. Any differences in section drags are not revealed in Fig. 15 and also can have only a relatively minor influence, in the same direction for both OHS and central-tail configurations, on the L/D values of Fig. 16, the final diagram. A corresponding comparison was also made between designs featuring conventionally located aft tails.

For the purposes of the OHS vs central-tail comparisons, simplified situations were considered, which are not necessarily representative of optima. For the OHS configuration a situation was postulated in which for the symmetric wing cross section the horizontal stabilizer lift coefficient was set at a value equal to half the wing lift coefficient for all lift coefficients. Hence, from the general moment-based equation derived earlier,[2]

$$C_{\mathrm{LTH}} = \frac{(a/c_w)C_{\mathrm{LW}} + C_{M(c/4)W} + (c_{\mathrm{TH}}S_{\mathrm{TH}}/c_wS_W)C_{M(c/4)\mathrm{TH}}}{(S_{\mathrm{TH}}/S_W)(L'/c_w - a/c_w)} \tag{3}$$

For cases involving symmetric wing and tail airfoils, this expression reduces to the form:

$$C_{\mathrm{LTH}} = \frac{(a/c_w)C_{\mathrm{LW}}}{S_{\mathrm{TH}}/S_W(L'/c_w - a/c_w)} \tag{4}$$

and hence

$$\frac{L'}{c_w} = \left(\frac{a}{c_w}\right)\left\{\frac{C_{\mathrm{LW}}S_W}{C_{\mathrm{LTH}}S_{\mathrm{TH}}} + 1\right\} \tag{5}$$

Evaluation of Eq. (5) for the prescribed ratio of $C_{\mathrm{LTH}}/C_{\mathrm{LW}} = 0.5$, $S_{\mathrm{TH}}/S_W = 0.3$, and $a/c_w = 0.4$ (the latter corresponds to a c.g. location of 0.65 c_w aft of the leading edge at the MAC station) leads to the result

$$L'/c_w = 3.0667$$

This dimensionless lever-arm distance from MAC/4 of the wing to MAC/4 of the horizontal stabilizer ensures that when $S_{\mathrm{TH}}/S_W = 0.3$, $a/c_w = 0.4$, $C_{\mathrm{LTH}}/C_{LW} = 0.5$ for all C_{LW} for a symmetrical airfoil. These values, therefore, justify the chain-dashed curve on Fig. 15 of C_{LTH} vs C_{LW}. Also when the performance prediction procedures outlined elsewhere[2] are invoked, the OHS performance, shown as a solid line on Fig. 16, can be evaluated for the special case involving symmetric wing and tail airfoil sections for a wing aspect ratio of 6 and an effective horizontal-stabilizer aspect ratio of 8, with $C_{\mathrm{LTH}}/C_{\mathrm{LW}} = 0.5$ when $a/c_w = 0.4$ and $S_{TH}/S_W = 0.3$.

For an OHS configuration employing a wing with an airfoil of asymmetric section, the effect of this is to reduce the value of C_{LTH}, for a prescribed c.g. location, $C_{M(c/4)W}$, and L'/c_w, as C_{LW} is reduced. Choosing a value of C_{LTH} equal to half the wing lift coefficient C_{LW}, such that the maximum and minimum values of C_{LTH} overshoot and undershoot the value of $C_{\mathrm{LTH}} = 0.5C_{\mathrm{LW}}$, respectively, by about equal amounts implies $C_{\mathrm{LTH}} = 0.5C_{\mathrm{LW}}$ when $C_{\mathrm{LW}} = 0.8$. For an asymmetric airfoil for which $C_{M(c/4)w}$ has an invariant value $= -0.15$, representative of a generic supercritical airfoil, with symmetric tail assembly airfoils, yields a moment equation of the form

$$C_{\mathrm{LTH}} = \frac{(a/c_w)C_{\mathrm{LW}} + C_{M(c/4)w}}{S_{\mathrm{TH}}/S_W(L'/c_w - a/c_w)} \tag{6}$$

Thus employing the same value of $S_{\mathrm{TH}}/S_w = 0.3$ as for the preceding case and moving the c.g. as far rearwards as possible as is consistent with maintaining an adequate static margin (0.24 c_w) and avoiding high structural stresses[3] implies a center of gravity no further aft than 80% of MAC. Hence when $a/c_w = 0.55$ and with $C_M(c/4)w = -0.15$, it can be shown that

$$L'/c_w = 2.9667$$

This results in the solid-line curve on Fig. 15 that is steeper than the chain-dashed line for the zero-moment case. Short length curves for $C_{M(c/4)w} = -0.3$ and -0.4 have also been added to Fig. 15 to represent the relationship between C_{LTH} and C_{LW} with hypothetical wing flaps deployed. The curve for $C_{M(c/a)W} = -0.15$ contributed to the dotted curve for OHS configurations presented in Fig. 16, again for a main-plane aspect ratio of 6 and an effective horizontal-stabilizer aspect ratio of 8. It can be seen that the dotted curve has a slightly better L/D for $0.8 \leq C_{LW} \leq 1.0$ because the value of $C_{\mathrm{LTH}}/C_{\mathrm{LW}}$ exceeds 0.5. In the range $0.4 \leq C_{\mathrm{LW}} \leq 0.8$, the value of L/D is lower than for the symmetrical wing-section case because of the ratio $C_{\mathrm{LTH}}/C_{\mathrm{LW}}$ being less than 0.5.

The results of the comparative performance predictions for aircraft with centrally located tails are presented in the lower set of curves displayed in Fig. 16. The solid curve relates to the use of a wing of symmetric section, and the wing pitching-moment coefficient about the MAC/4 station is, therefore, zero. The c.g. location was taken to lie at the MAC/4 station; hence, it was assumed that no lift, positive or negative, was required from the horizontal stabilizer surface to maintain level flight. The horizontal surface would, therefore, only serve for control purposes as would the single, centrally located, vertical surface. The areas of both the horizontal and vertical surfaces were each taken to be equal to 30% of the wing area.

The lower dashed curve is for a configuration employing, in conjunction with a centrally located aft-tail assembly, a wing of asymmetric section having a pitching-moment coefficient of -0.15 representative of a generic supercritical airfoil. The c.g. was, again, taken to be at the MAC/4 wing station. For this wing section a negative lift was required at the tail to counter the nose-down (negative) pitching moment of the wing. The negative lift, like the positive tail lift for the OHS cases, tended to inhibit the drag of the horizontal stabilizer but did penalize the mainplane with a requirement that the latter component had to generate sufficient additional lift to cancel out the negative tail-lift of the tail. Because of the assumed constancy of the wing pitching-moment coefficient, the negative tail-lift coefficient required to maintain level flight was also a constant and was, therefore, independent of C_{WL}.

Discussion

It is noteworthy that from the low-Reynolds-number tests of the wind-tunnel model, which also included tail-support booms and a minimalist fuselage for wind-tunnel mounting purposes, the L/D of the OHS model divided by that of the central tail version was 1.35. This is essentially identical with the value, for similar test conditions, found previously[1] using nonswept wings.

An even greater improvement, a ratio of about 1.5, was found at a much higher, but still modest, wing-chord-based Reynolds number of 9×10^6, when the presence of booms and fuselage were ignored. The analysis for this Reynolds number, which also differed in several small details from the conditions for the wind-tunnel tests, used standard NACA, experimentally obtained, airfoil data.

The magnitudes of the drag ratios for OHS vs conventional central tail configurations presented in Fig. 16 are explainable when appropriate account is taken of the thrust generation attributed to OHS tail surfaces. Collectively, the tails only contribute to drag at low C_{WL} values ($\cong 0.4$ or less). Thrust generation by the vertical surfaces is explainable much in the manner in which thrust generation by winglets is explained. However the horizontal tail surfaces also generate thrust in addition to contributing to lift and serving as stabilizers. The procedures used here for evaluating tail performances was similar to that described elsewhere,[2] which made use of experimental work, by McAlister and Takahashi, on wing-tip flows.[5] The latter material was reinforced using University of Calgary flow-visualization observations.[2]

The selection of wings of simple rectangular planform for OHS aircraft was made, originally, on the basis of structural considerations. However recent work on formation flying[6] implies that a wing of rectangular planform is more desirable than one of, say, elliptic planform because it improves the effectiveness of downstream surfaces. For the case of OHS configurations, these surfaces are the tail surfaces.

Some experimental work with the formation flying of two aircraft[7] suggests that the notable benefit in drag reduction experienced by the downstream aircraft might well be about equal to that obtainable from a single OHS aircraft after making due allowances for the boom and fuselage drags of the latter.

Conclusions

A low-speed, wind-tunnel, study showed that the OHS concept as such is applicable to swept-wing situations. For OHS aircraft wing sweep implies forward sweep rather than the customary, and familiar, aft-swept arrangement of conventional, central-tail-assembly configurations. It was also found that wing washout, from the tail support booms to the central fuselage, was important for achieving the best performance of swept-wing OHS aircraft and is comparable with the practice of imposing washout, from the central fuselage towards the wing tips, of conventional aft-swept wings. The inherent reasons for the imposition of washout on wings of invariant airfoil section are essentially the same for both aft- and forward-swept wings. The fractional performance improvement, in terms of lift/drag ratio, of swept OHS configurations compared with nonswept versions, in both cases employing wings of symmetric section, was essentially the same and, as derived from wind-tunnel tests, was 1.35 with, for the swept-wing case, a sweep angle of 25 deg. The comparative wind-tunnel tests with the rigid forward-swept wing in conjunction with a central tail assembly did not purport to represent, in model form, any feasible full-scale vehicle.

Because high-subsonic Mach-number aircraft are not likely to employ wings of symmetric cross section but, more probably, wings of the so-called supercritical type, a theoretical treatment was used to compare lift/drag performances of OHS with conventional configurations when both types employ symmetrical airfoil profiles and also with asymmetric wing sections with a relatively large pitching-moment coefficient of -0.15 representative of generic supercritical wings. It was shown by this means that the negative pitching moment degraded the performances of both the OHS and comparable conventional (central-tail-assembly) configurations, but the OHS configuration remained much superior over the range of wing lift coefficients investigated.

Acknowledgments

The first author acknowledges financial assistance from the Natural Sciences and Engineering Research Council of Canada for support from the Individual Research Grants Program.

References

[1]Kentfield, J. A. C., "The Case for Aircraft with Outboard Horizontal Stabilizers," *Journal of Aircraft*, Vol. 32, No. 2, 1995, pp. 398–403.

[2]Kentfield, J. A. C., "Influence of Aspect Ratio on the Performance of Outboard-Horizontal-Stabilizer Aircraft," *Journal of Aircraft*, Vol. 37, No. 1, 2000, pp. 62–67.

[3]Kentfield, J. A. C., "Structural Loading of Outboard-Horizontal Stabilizer Aircraft Relative to Comparable Conventional Designs," *Journal of Aircraft*, Vol. 38, No. 1, 2001, pp. 174–180.

[4]Kentfield, J. A. C., "The Aspect-Ratio Equivalence of Conventional Aircraft with Configurations Featuring Outboard Horizontal Stabilizers," *Journal of Aerospace*, SAE Transactions, Vol. 106, Sec. 1, 1997, pp. 1733–1741.

[5]McAlister, K. W., and Takahashi, R. K., "NACA 0015 Wing Pressure and Trailing Vortex Measurements," NASA TP-3151, 1991; also U.S. Army Aviation Systems Command, TR 91-A-003, 1991.

[6]Iglesias, S., and Mason, W. H., "Optimum Spanloads in Formation Flight," AIAA Paper 2002-0258, Jan. 2002.

[7]Iannotta, B., "Vortex Draws Flight Research Forward," *Aerospace America*, Vol. 40, No. 3, March 2002, pp. 26–30.